DOI 10.5012/bkcs.2010.31.5.1123

Articles

A Simple and Quick Chemical Synthesis of Nanostructured Bi_2Te_3, Sb_2Te_3, and $Bi_xSb_{2-x}Te_3$

HeeJin Kim, Ki Jung Lee,† Sung-Jin Kim,* and Mi-Kyung Han*

Department of Chemistry and Nano Science, Ewha Womans University, Seoul 120-750, Korea
**E-mail: sjkim@ewha.ac.kr (S. J. K.), mikihan@ewha.ac.kr (M-K. H.)*
†Northfield Mount Hermon School 12th, Massachusetts, USA
Received January 4, 2010, Accepted February 22, 2010

We report a simple and quick route for the preparation of high-quality, nearly monodisperse Bi_2Te_3, Sb_2Te_3, and $Bi_xSb_{2-x}Te_3$ nanocrystallites. The reactions of bismuth acetate or antimony acetate with Te in oleic acid result in pure phase of Bi_2Te_3 or Sb_2Te_3 nanoparticles, respectively. Also, ternary $Bi_xSb_{2-x}Te_3$ nanoparticles were successfully synthesized using the same method. The size and morphology of the nanoparticles were controlled by varying the stabilizing agents. The as-prepared nanoparticles are characterized by X-ray diffraction, scanning electron microscope, and high-resolution transmission electron microscope using an energy dispersive spectroscopy.

Key Words: Bi_2Te_3, Sb_2Te_3, $Bi_xSb_{2-x}Te_3$, Nanoparticle, Thermoelectric material

Introduction

Binary tellurides, such as Bi_2Te_3 and Sb_2Te_3, and their solid solutions are attracting much attention because of their applicability to room-temperature thermoelectric (TE) devices.[1-3] Ternary alloys of the bismuth-antimony system, such as $Bi_{0.5}Sb_{1.5}Te_3$, are being used in thermoelectric materials for coolers.[4] The performance of thermoelectric devices depends on the figure of merit (ZT, defined as $\sigma S^2T/\kappa$; where S is the Seebeck coefficient (or thermopower), σ electrical conductivity, κ thermal conductivity, and T is the temperature in Kelvin.) of the thermoelectric material.[5] Recent theoretical and experimental studies show that the use of thermoelectric materials comprising nanostructured components increases ZT relative to that of the bulk counterparts of these materials.[6-8] For example, Poudel *et al*. reported ZT = 1.4 for the p-type $Bi_xSb_{2-x}Te_3$ bulk alloy made by hot pressing the nanocrystalline powders.[1] It has been known that the existence of nano particles in bulk thermoelectric materials can improve ZT value. Furthermore, controlling the size and content of the nanoscale constituents within the bulk materials is expected to be important to achieve high ZT. [6-8] Thus, new routes for the preparation of these components as nanoscale powders are essential for incorporating them as nanoscale constituents of the bulk materials.

During the last few years, there have been many reports on the preparation of these materials in nanocrystalline form, using techniques, such as electrochemical deposition,[9-11] hydro/solvothermal synthesis,[12,13] colloidal processing[14-16] and microwave irradiation.[17,18] These methods for synthesizing nanostructured materials generally require prolonged heating or complex apparatus. Facile and mild routes to nanocrystalline tellurides in large quantities are desirable. Based on these views, we report a simple colloidal route for preparing of nearly monodisperse Bi_2Te_3, Sb_2Te_3 and $Bi_xSb_{2-x}Te_3$ nanocrystals at low temperature (below 150 °C) from a single reaction system. The influences of reaction temperature, reaction time, and the stabilizing agent on the formation of the nanoparticles have been systematically examined in these reaction systems.

Experimental

Bismuth acetate (99.99%), antimony acetate (99%), tellurium (99%), 1-dodecanethiol, oleic acid, trioctylphosphine(TOP) were used as received from Aldrich.

Synthesis of Bi_2Te_3 and Sb_2Te_3 nanoparticles. In a typical procedure, 2 mmol of bismuth acetate (antimony acetate for Sb_2Te_3) was dissolved in 20 mL oleic acid. The mixture was heated to 40 °C and held there for 30 min under vacuum and a transparent solution was obtained. After the flask was flooded with nitrogen, it was further heated to the desired reaction temperature (50 °C, 100 °C, and 150 °C). While holding the final temperature, Te-TOP solution, which was freshly prepared by dissolving 10 mmol Te powder in 10 mL TOP and 1 ml 1-dodecanethiol solution with rapid stirring for 2 hr at 160 °C under N_2, were rapidly injected into the flask. The reaction solution changed color from clear to black immediately after the injection of the TOP-Te source. Then the reaction was allowed to proceed for 1 min. After the reaction went to completion, the solution was cooled to room temperature by placing the flask in a water bath and then centrifuged at 18000 rpm for 30 min. The dark product was washed with acetone and dried in air at room temperature.

Synthesis of $Bi_xSb_{2-x}Te_3$ nanoparticles. A solid solution of $Bi_xSb_{2-x}Te_3$ nanoparticles was synthesized through a similar process. In a typical synthesis, 1 mmol of bismuth acetate and 1 mmol of antimony acetate were dissolved in 20 mL 1-dodecanethiol. The mixture was heated under vacuum to 40 °C and

held there for 30 min and a transparent yellow solution of oleate precursor was obtained. The flask was flooded with nitrogen and further heated to 100 °C, where Te-TOP (10 mmol Te in 10 mL TOP) was rapidly injected. The reaction was allowed to proceed for 1 min. The reaction solution color changed from clear yellow to black. After the reaction went to completion, the solution was cooled to room temperature using a water bath, and then centrifuged at 18000 rpm for 30 min. The dark product was washed with acetone and dried in air at room temperature. Two sets of the same experiment were repeated using (1) a mixture of 10 mL oleic acid and 10 mL 1-dedecanethiol, and (2) 20 mL oleic acid.

Characterization. The phase analysis and structural characterization of the material were carried out using powder X-ray diffraction. The data were collected on a Rigaku D/MAX X-ray (40 KV and 30 A) diffractometer with CuK_α ($\lambda = 1.54056$ Å). The particle morphology and size were determined by HR-TEM. Samples for TEM were prepared by evaporating a drop of the material suspended in hexane onto a carbon coated copper grid. The TEM images were recorded on HRTEM, JEOL 2100F. Selected area electron diffraction (SAED) patterns were obtained by TEM. Stoichiometry data were obtained from energy dispersive spectrometry. FE-SEM Images were collected using a JEOL (JSM -5800) with an accelerating voltage of 10 kV.

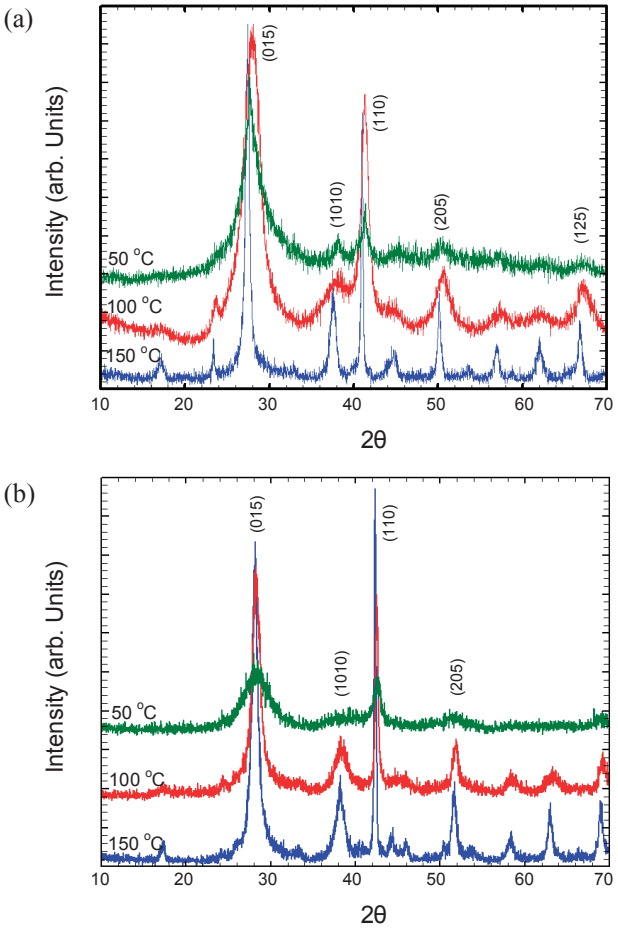

Figure 1. Powder XRD of (a) Bi_2Te_3, (b) Sb_2Te_3 obtained at different temperatures.

Results and Discussion

To validate the effect of reaction temperature on the formation of nanoparticles, we conducted a series of experiments under identical reaction conditions except for reaction temperatures (room temperature, 50 °C, 100 °C, and 150 °C). XRD patterns of Bi_2Te_3 and Sb_2Te_3 were collected for the products obtained at 50 °C, 100 °C and 150 °C. They are shown in Figure 1. We were unable to isolate decent product for reaction at room temperature.

Figure 1 shows XRD pattern of the products obtained at different temperatures. Temperature has the greatest impact on the crystallinity of particles. There are poorly resolved peaks. The significant broadening of the diffraction peak obtained at 50 °C and 100 °C indicates that the grain sizes of the sample are on the nanometer scale. The peaks become more intense and sharper

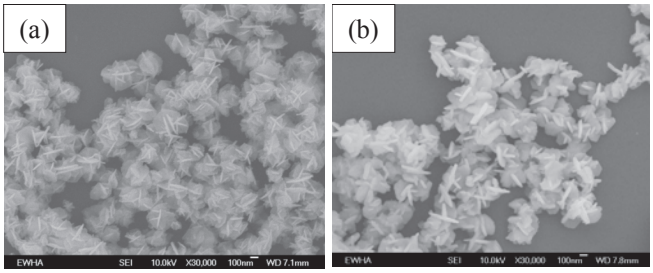

Figure 2. SEM images of (a) Bi_2Te_3, (b) Sb_2Te_3 obtained at 150 °C. All scale bars are equal to 100 nm.

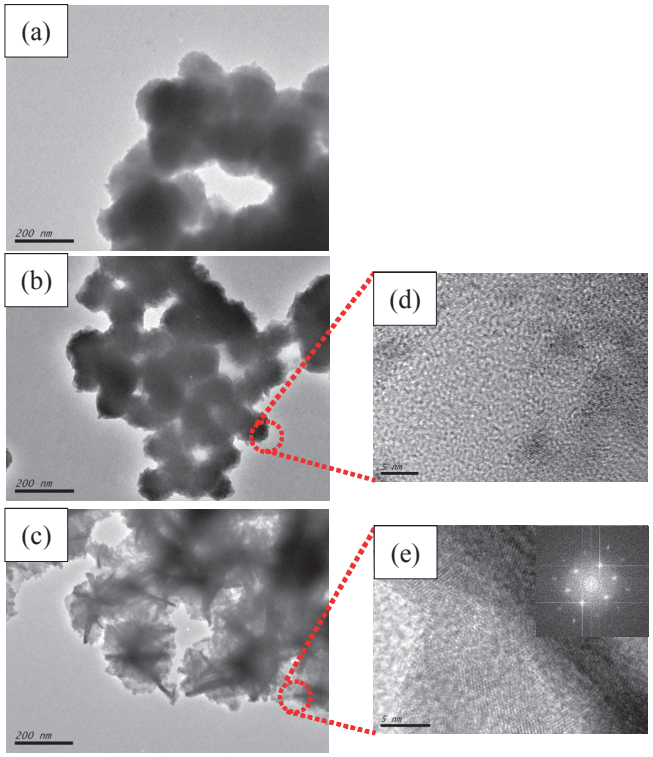

Figure 3. TEM image of Bi_2Te_3 obtained at (a) 50 °C, (b) 100 °C, and (c) 150 °C; (d) - (e) HRTEM image of the constituent nanoparticles of Bi_2Te_3 products obtained with inset of electron diffraction pattern.

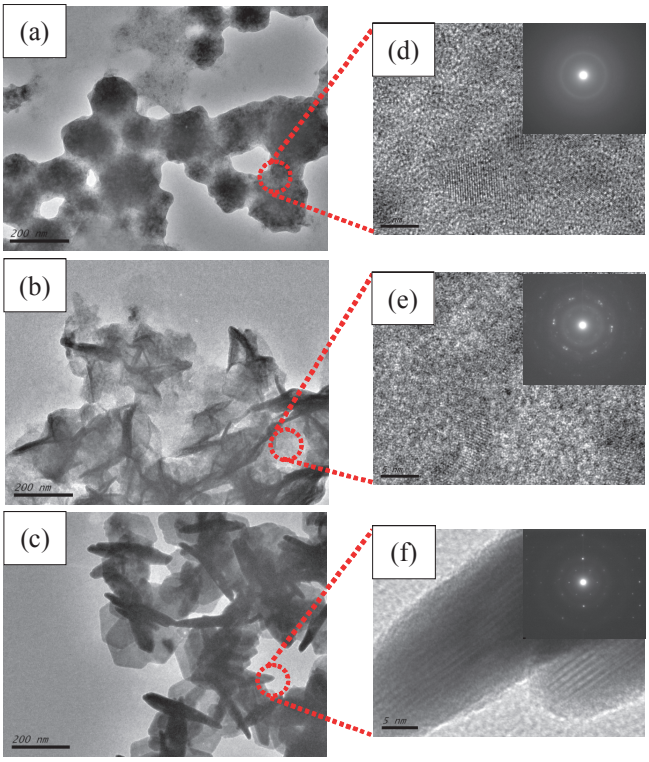

Figure 4. TEM image of Sb_2Te_3 obtained at (a) 50 °C, (b) 100 °C, and (c) 150 °C; (d) - (f) HRTEM image of the constituent nanoparticles of Bi_2Te_3 products with inset of electron diffraction pattern.

with an increase in the reaction temperature, indicating Bi_2Te_3 and Sb_2Te_3 nanocrystals are well crystallized and their particles sizes are growing larger. All of the diffraction peaks obtained at 150 °C can be indexed as the rhombohedral phase of Bi_2Te_3 and Sb_2Te_3. They are in agreement with the reported values (JCPDS, No. 15-0863 for Bi_2Te_3; JCPDS, No. 15-0874 for Sb_2Te_3).[19] No impurities were detected. The lattice constants can be refined as a = 4.405 (1) Å, c = 30.864 (7) Å for Bi_2Te_3 and a = 4.269 (1) Å, c = 30.660 (7) Å for Sb_2Te_3.

Further structural characterizations of the obtained particles were carried out using SEM and TEM. Figure 2 is the SEM images of the prepared Bi_2Te_3 and Sb_2Te_3 samples at 150 °C. It shows a large quantity of nanoparticles of uniform size/shape could be routinely obtained using this synthetic method.

Figure 3 shows TEM images of Bi_2Te_3 obtained at different temperatures. HRTEM images taken from the edge area of the particles are also shown in Figure 3 (d) and (e). For the synthesis of Bi_2Te_3 at 50 °C, the nanoparticles were amorphous phase only, which is consistent with the XRD analysis. When the reaction was carried out at 100 °C, nanoparticles with size 100 nm nanospheres were obtained. Interestingly, the HRTEM image of the edge of a single nanoparticle reveals that the Bi_2Te_3 nanoparticles consist of primary crystalline nanoparticles with a size of 3 ~ 5 nm (shown in Figure 3 (d)). Then at a reaction temperature of 150 °C, the material has a wafer like morphology, shown in Figure 3 (c). Both HRTEM and SAED show that these wafers have an increased crystallinity, in agreement with the XRD results.

Meanwhile, Figure 4 shows TEM images of Sb_2Te_3 obtained

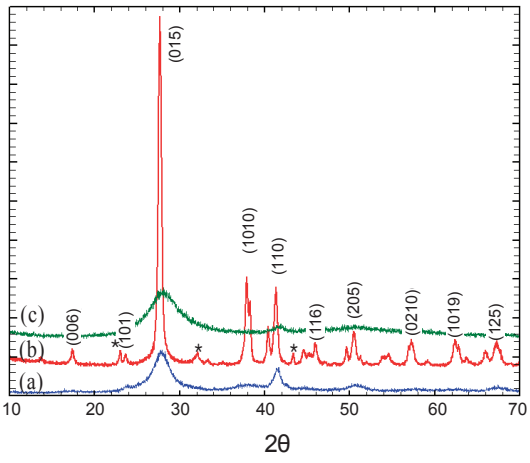

Figure 5. Powder XRD patterns of $Bi_xSb_{2-x}Te_3$ nanocrystals synthesized using different stabilizing agents of (a) oleic acid only, (b) oleic acid and 1-dodecanethiol, and (c) 1-dodecanethiol only.

at different temperatures. HRTEM images taken from the edge area of the particles are also shown in Figure 4 (d)-(f). The HRTEM image obtained from the edge of an Sb_2Te_3 nanoparticle shows that constituent nanoparticles 5 ~ 7 nm in size are observed at a temperature lower than the temperature of the Bi_2Te_3 system. The morphological evolution of Sb_2Te_3 can be clearly observed at the reaction temperature of 150 °C. As shown in Figure 4 (f), the particles show excellent crystallinity and very well defined facets. Well-defined lattice fringes were also observed and the electron diffraction image shown in the inset of this figure reveals clear diffraction spots that correspond to the hexagonal phase of Sb_2Te_3.

$Bi_xSb_{2-x}Te_3$. Because the best materials for thermoelectric cooling applications are found among the solid solutions of Bi_2Te_3 with Sb_2Te_3, the same synthetic procedure with mixed precursors was conducted to prepare a ternary system having the composition $BiSbTe_3$. Based on the above experimental results, it is necessary to control the reactivity of Bi and Sb from a single reaction system to prepare the solid solution of Bi_2Te_3 with Sb_2Te_3. In the present work, the influence of the stabilizing agent, oleic acid and/or 1-dodecanethiol, is examined, while other reaction conditions are held steady.

XRD patterns of $Bi_xSb_{2-x}Te_3$, shown in Figure 5, were collected for the products obtained from the three different sets of experiments; namely, reaction at 100 °C, using (A) 20 mL oleic acid only, (B) 10 mL oleic acid and 10 mL 1-dodecanethiol, and (C) 20 mL 1-dodecanethiol only. The XRD pattern of $Bi_xSb_{2-x}Te_3$ in Figure 5 shows that the stabilizing agents have significant influence on the crystallinity and size of $Bi_xSb_{2-x}Te_3$ nanocrystals. When the stabilizing agent is either oleic acid or 1-dodecanethiol, the crystallinity of the products is poor. However, the XRD peaks of the product become more intense and narrow for the reaction in which both stabilizing agents are present. All diffraction peaks can be indexed as rhombohedral phase with lattice parameters a = 4.374(1) Å and c = 30.499 (4) Å. Additional weak peaks observed at 2θ = 23.1, 32.3 and 43.2° are those of Te elements. In view of the atomic radii of Bi and Sb (117 pm and 90 pm), the values obtained for the lattice

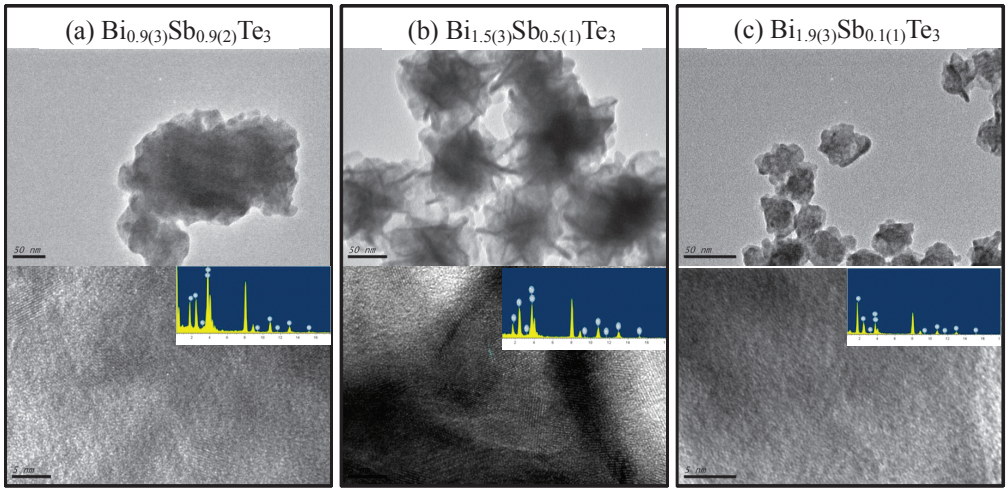

Figure 6. TEM images of $Bi_xSb_{2-x}Te_3$ nanocrystals synthesized using stabilizing agent of (a) oleic acid only, (b) oleic acid and 1-dodecanethiol, and (c) 1-dodecanethiol only : (TOP) low magnification TEM image. All scale bars are equal to 50 nm, (BOTTOM) HRTEM image of a part of a crystal with inset of EDS showing that the average atomic ratio of compositions. All scale bars are equal to 5 nm.

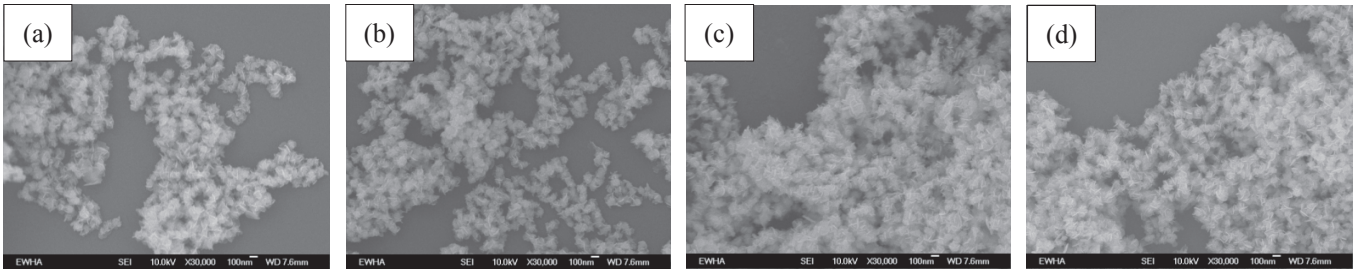

Figure 7. FE-SEM image of $Bi_xSb_{2-x}Te_3$ nanocrystals obtained at 100 °C for (a) 5 min, (b) 30 min, (c) 2 hr, and (d) 18 hr.

parameters are in fair agreement with JCPDS data for bulk $BiSbTe_3$.[19]

The morphologies of the nanostructured $Bi_xSb_{2-x}Te_3$ were examined by TEM. Figure 6 shows the TEM observation of $Bi_xSb_{2-x}Te_3$ nanocrystals synthesized under different synthetic conditions. For the reaction using only one stabilizing agent, oleic acid, the composition of the nanoparticles was further analyzed by EDS, (shown in Figure 6 insets), in which the atomic ratio of Bi : Sb : Te was found to be approximately 0.9 (3) : 0.9 (2) : 3.0, $Bi_{0.9(3)}Sb_{0.9(2)}Te_3$. Under this condition, large irregular particles were formed. The HRTEM image of the edge of the particle shows that each particle consists of primary crystalline nanoparticles, shown in Figure 6 (a) BOTTOM. Figure 6 (b) shows the morphology of these particles when a mixture of 1-dodecanethiol and oleic acid is used in the reaction. The shapes of the particles are similar to those of Bi_2Te_3. The average size of the particles is ~130 nm. Well-defined lattice fringes were observed. The composition of the nanoparticles as calculated from the EDS spectrum gives an Bi : Sb : Te atomic ratio of 1.5 (3) : 0.5 (1) : 3, as shown in Figure 6 (b). But the reaction using 1-dodecanethiol as the stabilizing agent gave smaller particles (average size ~45 nm). The atomic ratio of this nanoparticle obtained from the EDS spectrum is Bi : Sb : Te = 1.9 (3) : 0.1 (1) : 3, as shown in Figure 6 (c). It is likely that the coordinating ability of sulfur of 1-dodecanethiol differs from that of oxygen of oleic acid. Therefore, in going from the sulfide ligand of 1-dodecanethiol to the oxide ligand of oleic acid, the surface energies of the particles are modified and consequently influence their growth rates and compositions.

We observed that the composition and size of the particles can be controlled by choosing the proper stabilizing agent. A reaction using both stabilizing agents produces well defined larger nanoparticles than a reaction using only one stabilizing agent. The specific formation mechanism of $Bi_xSb_{2-x}Te_3$ under our experimental conditions is not yet clear and warrants further investigation.

The reaction was also carried out with variations in reaction time. The SEM images in Figure 7 show the morphology of $Bi_xSb_{2-x}Te_3$ nanoparticles synthesized at 100 °C for different reaction times. These particles have uniform diameters of approximately 200 nm regardless of reaction time. The SEM results demonstrate that reaction time weakly affects crystal growth and the phase formation of $Bi_xSb_{2-x}Te_3$ particles in this synthetic condition.

Conclusion

We have established a facile synthetic approach to nano-sized powders of Bi_2Te_3, Sb_2Te_3, and $Bi_xSb_{2-x}Te_3$. It is found that the reaction temperatures show the greatest impact on the cry-

stallinity of Bi_2Te_3 and Sb_2Te_3 particles. The composition of prepared $Bi_xSb_{2-x}Te_3$ nanoparticles can be controlled by varying the stabilizing agents. This method requires no complex apparatus or technique and the reaction is quite mild and convenient, which makes it suitable for the production of thermoelectric nanoconsituents on a large scale. As a follow-up, we are investigating the thermoelectric properties of the composites comprising these nanoparticles.

Acknowledgments. This research was supported by a grant (code #: 2009K000451) from 'Center for Nanostructured Materials Technology' under '21st Century Frontier R&D Programs' of the Ministry of Education, Science and Technology. M. Han acknowledges financial support from Basic Science Research Program through the National Research Foundation of Korea (NRF) funded by the Ministry of Education, Science and Technology, Korea.

References

1. Poudel, B.; Hao, Q.; Ma, Y.; Lan, Y.; Minnich, A.; Yu, B.; Yan, X.; Wang, D.; Muto, A.; Vashaee, D.; Chen, X.; Liu, J.; Dresselhaus, M. S.; Chen, G.; Ren, Z. *Science* **2008**, *320*, 634.
2. Ma, Y.; Hao, Q.; Poudel, B.; Lan, Y.; Yu, B.; Wang, D.; Chen, G.; Ren, Z. *Nano Lett.* **2008**, *8*, 2580.
3. Dirmyer, M. R.; Martin, J.; Nolas, G. S.; Sen, A.; Badding, J. V. *Small* **2009**, *5*, 933.
4. Zhao, Y.; Burda, C. *ACS Appl. Mater. Interfaces* **2009**, *1*, 1259.
5. Rowe, D. M. *CRC Handbook of Thermoelectrics*; CRC Press: LLC, 1995.
6. Venkatasubramanian, R.; Slivola, E.; Colpitts, T.; O'Quinn, B. *Nature* **2001**, *413*, 597.
7. Harman, T. C.; Taylor, P. J.; Walsh, M. P.; LaForge, B. E. *Science* **2002**, *297*, 2229.
8. Cheele, M.; Oeschler, N.; Meier, K.; Kornowski, A.; Klinke, C.; Weller, H. *Adv. Funct. Mater.* **2009**, *19*, 3476.
9. Lim, J. R.; Whitacre, J. F.; Fleurial, J.-P.; Huang, C.-K.; Ryan, M. A.; Myung, N. V. *Adv. Mater.* **2005**, *17*, 1488.
10. Li, S.; Soliman, H. M. A.; Zhou, J.; Toprak, M. S.; Muhammed, M.; Platzek, D.; Ziolkowski, P.; Mueller, E. *Chem. Mater.* **2008**, *20*, 4403.
11. Li, G.-R.; Zheng, F.-L.; Tong, Y.-X. *Cryst. Growth Des.* **2008**, *8*, 1226.
12. Xu, Y.; Ren, Z.; Ren, W.; Deng, K.; Zhong, Y. *Mater. Lett.* **2008**, *62*, 763.
13. Xu, Y.; Ren, Z.; Ren, W.; Cao, G.; Deng, K.; Zhong, Y. *Mater. Lett.* **2008**, *62*, 4273.
14. Sun, T.; Zhao, X. B.; Zhu, T. J.; Tu, J. P. *Mater. Lett.* **2006**, *60*, 2534.
15. Christian, P.; O'Brien, P. *J. Mater. Chem.* **2005**, *15*, 3021.
16. Purkayastha, A.; Kim, S.; Gandhi, D. D.; Ganesan, P. G.; Borca-Tasciuc, T.; Ramanath, G. *Adv. Mater.* **2006**, *18*, 2958.
17. Zhou, B.; Zhao, Y.; Pu, L.; Zhu, J.-J. *Mater. Chem. Phys.* **2006**, *96*, 192.
18. Yao, Q.; Zhu, Y.; Chen, L.; Sun, Z.; Chen, X. *J. Alloys Compd.* **2009**, *481*, 91.
19. McClune, W. *Powder Diffraction File, JCPDS International Center for Diffraction Data*, Swarthmore, PA.